Proposed Nonlinear Resonance Laser Technique for Manipulating Nanoparticles

Tetsuhiro Kudo* and Hajime Ishihara

Department of Physics and Electronics, Osaka Prefecture University, Sakai, Osaka 599-8531, Japan

(Received 4 May 2011; revised manuscript received 28 December 2011; published 24 August 2012)

We propose nonlinear resonant laser manipulation, a technique that drastically enhances the number of degrees of freedom when manipulating nano-objects. Considering the high laser intensity required to trap single molecules, we calculate the radiation force exerted on a molecule in a focused laser beam by solving the density matrix equations using the nonperturbative method. The results coherently elucidate certain recently reported puzzling phenomena that contradict the conventional understanding of laser trapping. Further, we demonstrate unconventional forms of laser manipulations using ''stimulated recoil force'' and ''subwavelength laser manipulation.''

DOI: 10.1103/PhysRevLett.109.087402 PACS numbers: 78.67.Bf, 42.65.−k, 78.20.N−, 78.40.−q

Laser manipulation (LM) is a technique for the mechanical control of small objects ranging in size from micrometers to nanometers using the radiation force (RF). Since its demonstration by Ashkin *et al.* [1,2], this technique has been developed for manipulating micron-sized objects (in the form of laser tweezers) in various research fields such as biochemistry, materials engineering, and micromachining [3–7]. The RF is divided into the dissipative (scattering and absorbing) force (DF) and the gradient force (GF). The DF is caused by a transfer of kinetic momentum from a photon to a target. The GF is due to the electromagnetic interaction with the light field and induced polarization. In the laser tweezers, a focused laser beam traps small objects using the GF.

The targets of LM have recently been shifted to nanoscale objects such as single organic molecules [8–12]; this introduces challenges because the RF exerted on these targets is extremely small. We have previously proposed the use of LM utilizing the electronically resonant optical response of nanostructures both to enhance the RF and to select particular kinds of nanoparticles (via quantum confinement) [13]. As theoretically demonstrated, this scheme is effective both for traveling and for standing waves [13,14]; its ability to move nanoparticles has been experimentally verified [15]. On the other hand, the use of resonance is considered to be difficult in trapping by a single focused laser beam because the resonantly enhanced DF pushes objects away from the focal point, according to the usual explanation of the trapping mechanism [16]. However, recent experiments using resonance focused laser beams have reported very positive results for molecular trapping [10–12] (case 1). Additionally, these studies [8,9,11] show certain puzzling phenomena that contradict the conventional interpretation of laser trapping based on the linear response theory [16,17]. For example, a significant increase in the trapping time of fluorophore-labeled antibodies when using resonant laser light has been reported [11], wherein the antibodies are trapped in an energy region above the resonance level of fluorophores, although under normal conditions, trapping is possible only at the energy below the resonance (at least in the conventional explanation of trapping mechanism) (case 2). Similarly, it was observed that trapping at energies above the resonance energy is several times more effective than that at levels below the resonance energy for the same molecules [9] (case 3). The demonstration by Hosokawa *et al.* is more extreme: the trapping time is substantially increased by the addition of a resonant laser (at 532 nm wavelength) whose intensity is weaker by several orders of magnitude than that of the main nonresonant trapping laser (at 1064 nm wavelength) [10] (case 4).

The key concept required to understand these phenomena is nonlinear optical response. It should be noted that the laser intensity in single molecular trapping, mentioned above, is always very strong and is beyond the perturbative nonlinear regime (this fact changes the scenario from the one used in the conventional explanation of the laser trapping). In this Letter, we propose nonlinear resonant laser manipulation. By considering the laser in the nonlinear regime, we can comprehensively elucidate the above mentioned puzzling effects found recently in molecular trapping studies (cases 1–4) and further drastically enhance the number of degrees of freedom in which we can manipulate nano-objects. For example, we demonstrate unconventional manipulations such as an optical aspiration by the stimulated recoil force, which pulls nanoparticles using traveling waves, and subwavelength laser manipulation beyond the diffraction limit. These demonstrations renovate the conventional understanding of laser trapping of nanoscale objects, which is in a rather different direction from the extension of the atom cooling scheme by considering nonlinear optical processes [18].

For our theoretical demonstrations, we start from the expression of the time averaged RF exerted on neutral matter, as written in [19]

$$\langle \mathbf{F}(\omega) \rangle = (1/2)\mathrm{Re} \int d\mathbf{r} [\nabla \mathbf{E}(\mathbf{r}, \omega)^*] \cdot \mathbf{P}(\mathbf{r}, \omega), \quad (1)$$

where $\mathbf{E}$ is the time harmonic electric field, and $\mathbf{P}$ is the induced polarization on a molecule. To calculate $\mathbf{P}$, we solve the standard matter density-matrix equations with the Hamiltonian $H = H_0 + V$. Here, H_0 is the unperturbed component, and V is the light-molecule interaction energy, which is given by $V = -\vec{\mu} \cdot \mathbf{E}(\mathbf{r}, t)$, where $\vec{\mu}$ is the dipole moment matrix. In this calculation, we use an incident field $\mathbf{E}_0$ for $\mathbf{E}$ because the effect of the scattered field is negligible in this case [20]. We assume the diagonal element of $\vec{\mu}$ to be zero. We consider up to two kinds of frequencies as incident fields, namely, $\mathbf{E}_0(\mathbf{r}, t) = \mathbf{E}_1(\mathbf{r}, \omega_1)\exp(-i\omega_1 t) + \mathbf{E}_2(\mathbf{r}, \omega_2)\exp(-i\omega_2 t) + \text{c.c.}$ Here, $(\mathbf{E}_1, \omega_1)$ and $(\mathbf{E}_2, \omega_2)$ are the amplitude and frequency of the first and second beams, respectively. To consider the strong excitation regime, we take the nonperturbative approach to solve the density-matrix equations and include the phenomenological relaxation constants used in Ref. [21]. We expand the off-diagonal elements of the density matrix in a Fourier series of the form $\rho_{nm}(\mathbf{r}, t) = \sum_{j,k} \rho_{nm}^{(j,k)}(\mathbf{r}, \omega_1, \omega_2)\exp[-i(j\omega_1 + k\omega_2)t] + \text{c.c.}$, where n, m, j, k are integers and the diagonal elements are limited to the lowest order in the same expansion. After substituting these equations into the density-matrix equations, we use the steady state approximation. Substituting resultant $\mathbf{P}$ into Eq. (1), which is the general formula of RF, along with $\mathbf{E}$, we obtain the RF $\langle \mathbf{F} \rangle$ exerted on a molecule [20].

For this calculation, by using angular spectrum representation [22], we assume a tightly focused laser beam that is in the diffraction limit. We assume that the light propagation and polarization are along z and x axes, respectively, and the focal point is set to be the origin. The numerical aperture (NA) of an oil immersion objective lens is 1.3 and the focal length and incident beam diameter are 1.6 mm and 1.3 mm, respectively, as indicated in Ref. [8]. In the calculation of RF, we consider two different positions where a molecule is located. Position 2 is in the vicinity of the usual trapping points, i.e., $z = +300$ nm on the z axis where the GF becomes almost maximum. Position 1 is on the negative side of the z axis and the distance from the origin is about ten times longer than that between the origin and the position 2, where the GF toward the focal center becomes weak enough. Regarding the target of the manipulation, we consider a typical organic molecule, for example rhodamine, with the vibrational excited levels illustrated in the inset of Fig. 1(a). For the parameters for the dipole moment μ_{nm} and resonance energies $\hbar\omega_{nm}$ of the molecule, we choose the values according to the kinds of molecules. We assume population decay times for the 3-2 state transition, and the 2-1 state transition of 3 ps and 4 ns, respectively (that of the 3-1 state transition is ignored). However, for a single molecule, definite values both for the dephasing constants of molecular excited states and for the background dielectric constant of the molecules are uncertain. Therefore, we examine these values within a certain range. Radius a of the organic molecule ($a = 1$ nm) is one order of magnitude larger than that of the water molecule, which allows us to use the high-frequency dielectric constant of the water molecule (1.77 is used in the present calculation).

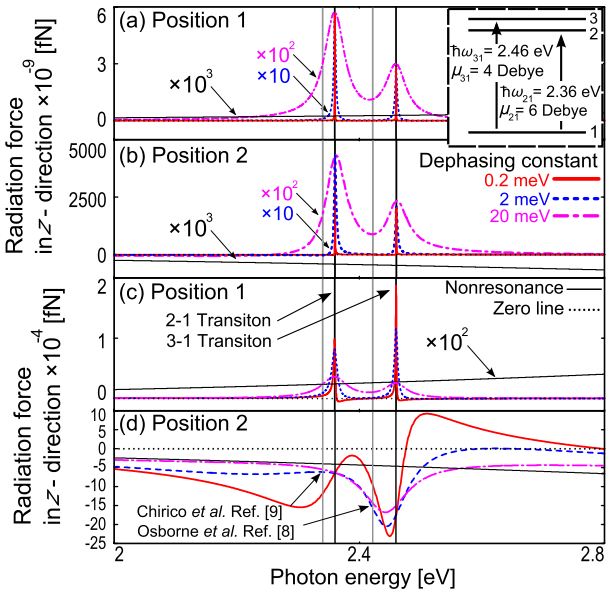

FIG. 1 (color online). Photon energy dependence of the RF along the z direction for several values of dephasing constant (0.2 meV, 2 meV, and 20 meV). A molecule with vibration levels [see inset of (a)] is assumed. (a) and (b) are for positions 1 and 2, respectively, under weak excitation (1 nW); (c) and (d) are for positions 1 and 2, respectively, under strong excitation (1 mW). Thin solid black lines indicate the nonresonant case. 2-1 and 3-1 transition energies are pointed by arrows in (c). Likewise, photon energies employed in the experiments of Ref. [8,9] are indicated in (d).

First, we observe the intensity dependence of the RF spectrum when the target is irradiated by the tightly focused laser beam. Figure 1(a) shows the spectra for the weak excitation intensities (1 nW). When the molecule is far from the focal point (position 1), the DF pushing the molecule toward the focal point is much stronger in the resonant case than in the nonresonant case. At position 2, where the molecule is pulled toward the focal point in the normal (nonresonant) case, DF is also dominant; the molecule is strongly pushed away from the focal point in the resonant case [Fig. 1(b)], which is thought to be the origin of the difficulty of resonant trapping. Moreover, the reduction in the RF by an increase in the dephasing constant is significant. On the other hand, in the strong excitation regime, this situation is drastically different. We choose 1 mW for the incident intensity. For the simple two-level system, the increase in the DF with incident intensity is known to be suppressed by the saturation effect, which has been shown for the atom case [23]. However, as shown in Refs. [16,23], the increased rate of GF appearing just below the resonance energy is not greatly suppressed; the peak width becomes broad because of saturation. As a

result, the GF becomes larger than the DF and the energy region for effective trapping becomes much wider [16] (no figure is shown in this text). The situation for the three-level system is more extreme, as shown in Fig. 1(d). We can see that the strong trapping force appears at energies just "above" the resonance level because **E** and **P** become in phase in contrast with the normal case due to the inverted population at the second level. While at position 1 [Fig. 1(c)], the pushing force (DF) is still dominant; it is much stronger than the nonresonant force. The molecules farther away drift much more strongly toward the focal point in the resonant condition. These results indicate that more rapid gathering of molecules can be induced using a strong focused beam and the resonance effect (case 1). In Ref. [9], Chirico *et al.* discussed the trapping efficiency in rhodamine 6G at higher energy levels, as demonstrated by Osborne *et al.* [8]; efficiency was four times greater than that at lower energy levels, as found by Chirico *et al.* Furthermore, the laser frequency was also between the 2-1 and 3-1 transitions in Ref. [11]. This situation is well explained by Fig. 1(d) (case 2). Although the efficiency values and the magnitudes of calculated trapping force cannot be directly compared, the calculated results in this study that use realistic parameters for rhodamine correctly reproduce the essential profile of the experimental results discussed by Chirico *et al.* (case 3) [see the arrows indicating corresponding energies above and below the resonance energy in Fig. 1(d)]. In Figs. 1(c) and 1(d), it is also interesting to note that the force spectra are not very sensitive to the dephasing constant in the strong nonlinear regime. This is because the peak width is primarily influenced by the saturation effect.

Next, we consider RF using two beams (here we term "532 nm laser" and "1064 nm laser") as used in Ref. [10]. The NA is assumed to be 1.25 for these beams. In this case, we consider the induced transition assuming the energy levels shown in the inset of Fig. 2, namely, the 532 nm laser induces excitation from the second level to the third level under illumination by the 1064 nm laser. In the experiment in Ref. [10], it was shown that the assistance of the 532 nm laser extends the averaged trapping time of the dye-doped polystyrene latex nanoparticles by several fold (case 4). In the present demonstration, we treat a bare single molecule as a target in order to focus on the essential mechanism of the proposed effect. We assume the dephasing constant of 0.2 meV and population decay times between the 3-1, 2-1, and 3-2 states of approximately 40, 4, and 3 ns, respectively. (We show the corresponding calculations for the case of dye-doped polystyrene latex nanoparticles used in Ref. [10] in the Supplemental Material [20], where we reproduce experimentally obtained trapping times by employing some assumed parameters and a more detailed level scheme of molecules.) Figure 2 shows the position dependence of the RF for the optimum photon energies of the two lasers (determined from the RF spectrum shown in the Supplemental Material [20]). From this result, we can

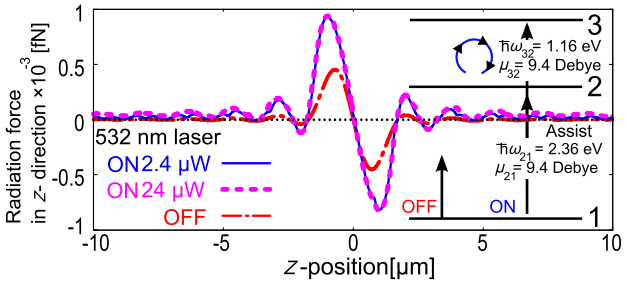

FIG. 2 (color online). Position dependence of the RF in the z direction scanned along the z axis. The solid blue and broken pink lines denote the case of assistance by a 532 nm laser at an intensity of 2.4 μW and 24 μW, respectively, under the illumination of a 1064 nm laser at an intensity of 5 mW. The long dashed dotted red line shows the nonresonant case of a 1064 nm laser at 5 mW. The inset shows the energy diagram of the target molecule.

see that the trapping force becomes approximately twice as large, when the 532 nm laser at 2.4 μW is simultaneously applied with the 1064 nm laser. This is particularly effective because the intensity of the assisting beam is three orders of magnitude weaker than the original trapping 1064 nm laser. Also we examine 24 μW for the 532 nm laser. Although the increase in the RF with the intensity of the 532 nm laser is saturated (as seen here) if its intensity is strong enough, we can say that this increase is very rapid as we need to add more 5 mW of the 1064 nm laser intensity if we want to double the magnitude of the RF solely by controlling the intensity of the 1064 nm laser.

Although we should require more detailed information regarding single molecular dephasing and microscopic influences from surrounding water molecules to allow quantitatively accurate derivation of the RF, we should note that the above demonstrations (with reasonable assumptions) coherently elucidate the central profile of the existing experimental results. This result strongly suggests the potentiality of nonlinear LM to diversely extend the number of degrees of freedom to allow mechanical control of nano-objects. In what follows, we show some examples of this kind of extension of the LM technique.

First, we demonstrate the "stimulated recoil force" that can be used to pull the nano-objects using a traveling wave. The configuration of the laser beams and the nano-object under consideration is given in the inset of Fig. 3. Assuming the same energy levels of the particle as those shown in the inset of Fig. 1(a), we irradiated a particle with a standing wave to create the inversion of the population and sent another laser beam along the direction perpendicular to the standing wave. The intensity of the lasers was 100 kW/cm^2; the polarization direction is assumed to be common for those beams. In the absence of the pumping standing wave, the traveling wave exerts the usual DF to push the particle (broken blue line in Fig. 3). Under the strong irradiation of the standing wave, however, the

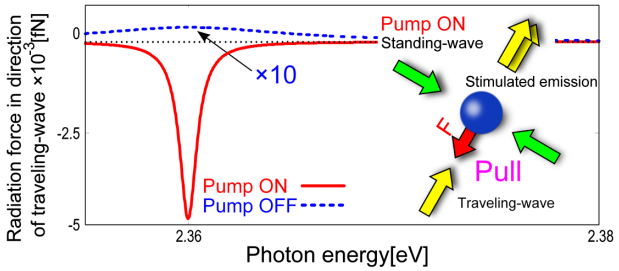

FIG. 3 (color online). Spectra of the RF along the direction of the traveling wave. The solid red and broken blue lines are the cases when the target is irradiated and not irradiated by the standing wave. The inset shows a schematic diagram of the "stimulated recoil force." In the present calculation, the standing wave's photon energy is fixed at the 3-1 transition energy.

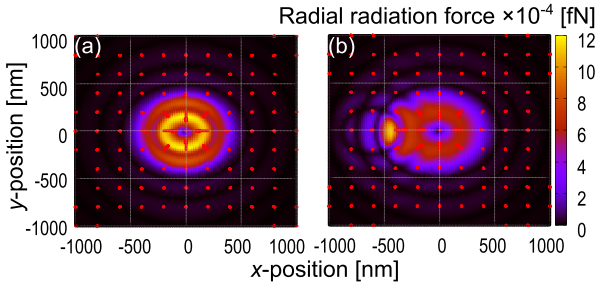

FIG. 4 (color online). Spatial map of the RF in the radial direction in the x-y plane induced by 532 and 1064 nm laser beams. We centered the 1064 nm laser beam at $(x, y) = (0, 0)$ and centered the 532 nm laser beam at (0,0) (a) and at ($-$ 600 nm, 0) (b). The arrows represent the direction of the RF.

direction of force reverses. In this event, two photons with the same mode as the incident one are emitted via stimulated emission, and hence, the momentum conservation law requires the particle to have the opposite momentum from that of the incident photon. This demonstration indicates that quantum optical effects greatly increase the potential of LM. Further, the "pulling" operation clearly raises the number of degrees of freedom and increases the RF used to manipulate small particles relative to the "pushing" operation.

The next example shows the manner in which the nonlinear regime offers great technical advantages to LM. The mechanism used to enhance RF is the assistance of a weak resonant laser (Fig. 2). The same kind of molecule as that shown in Fig. 2 is the trapping target. In Fig. 4(b), we can see that the area of the prominent force becomes narrower than that in Fig. 4(a), where we select the optimum energy of the two beams. As the extra force from the assisting beam works only in the beam overlap area, we can provide a method to realize "subwavelength laser manipulation" beyond the diffraction limit without using near field optical force [5]. This mechanism is based on the similar concept of ultraresolution optical microscopy [24] using two beams.

Finally, we wish to remark that the calculation under ideal conditions tends to result in an underestimated RF, as pointed out in [8]. On the other hand, some reports suggest the operation of nonequilibrium dynamics in the solvent [25] and demonstrate the dynamics simulation of a nanoparticle's motion under free thermal diffusion [26]. These observations indicate that the evaluation of realistic molecular motion by a focused beam requires the inclusion of information (specifically, on certain parameters of the single molecule and the dynamics of the solvent) into the theoretical model. This will be a challenge in our future study. However, in such a study, the findings of the present study, that is, deriving RF from the nonlinear response, will play a central role in providing significant profiles of nanoparticle dynamics and strongly encourage us to use the nonlinear regime to increase the number of degrees of freedom so as to mechanically manipulate nano-objects.

In conclusion, we have proposed the nonlinear resonant laser manipulation technique by considering the nonlinear optical effect beyond the perturbative regime; we can comprehensively elucidate recently reported effective trapping and puzzling phenomena contradicting the conventional explanation of the mechanisms of laser trapping. Recently, peculiar trapping of metal particles by nonlinear effects has been reported [27]. Although it is not a resonant case, this result suggests that the development of LM technology under the heading of "nonlinear response" will become a reality in the near future.

The authors thank Professor H. Masuhara, Professor Y. Tsuboi, Professor T. Sugiyama, and Dr. T. Shoji for their fruitful discussions. This work was partially supported by the Grant-in-Aid for Scientific Research (KAKENHI) No. 19049014 on Priority Area "Strong Photons-Molecules Coupling Fields (470)" from the Ministry of Education, Culture, Sports, Science and Technology (MEXT) of Japan and the Japan Society for Promotion of Science (JSPS).

*kudo@pe.osakafu-u.ac.jp

[1] A. Ashkin, Phys. Rev. Lett. **24**, 156 (1970).
[2] A. Ashkin, J. M. Dziedzic, J. E. Bjorkholm, and S. Chu, Opt. Lett. **11**, 288 (1986).
[3] T. T. Perkins, D. E. Smith, and S. Chu, Science **264**, 819 (1994).
[4] M. P. MacDonald, G. C. Spalding, and K. Dholakia, Nature (London) **426**, 421 (2003).
[5] A. H. J. Yang, S. D. Moore, B. S. Schmidt, M. Klug, M. Lipson, and D. Erickson, Nature (London) **457**, 71 (2009).
[6] F. M. Fazal and S. M. Block, Nature Photon. **5**, 318 (2011); K. Dholakia and T. Čižmár, Nature Photon. **5**, 335 (2011); M. Padgett and R. Bowman, Nature Photon. **5**, 343 (2011).
[7] S. Ito, Y. Tanaka, H. Yoshikawa, Y. Ishibashi, H. Miyasaka, and H. Masuhara, J. Am. Chem. Soc. **133**, 14472 (2011).

[8] M. A. Osborne, S. Balasubramanian, W. S. Furey, and D. Klenerman, J. Phys. Chem. B **102**, 3160 (1998).
[9] G. Chirico, C. Fumagalli, and G. Baldini, J. Phys. Chem. B **106**, 2508 (2002).
[10] C. Hosokawa, H. Yoshikawa, and H. Masuhara, Jpn. J. Appl. Phys. **45**, L453 (2006).
[11] H. Li, D. Zhou, H. Browne, and D. Klenerman, J. Am. Chem. Soc. **128**, 5711 (2006).
[12] Y. Tsuboi, T. Shoji, M. Nishino, S. Masuda, K. Ishimori, and N. Kitamura, Appl. Surf. Sci. **255**, 9906 (2009).
[13] T. Iida and H. Ishihara, Phys. Rev. Lett. **90**, 057403 (2003); Phys. Rev. B **77**, 245319 (2008); see also, Phys. Rev. Focus, 11, story 6, 11 February 2003; and Phys. Rev. Focus, 21, story 21, 25 June 2008.
[14] H. Ajiki, T. Iida, T. Ishikawa, S. Uryu, and H. Ishihara, Phys. Rev. B **80**, 115437 (2009).
[15] K. Inaba, K. Imaizumi, K. Katayama, M. Ichimiya, M. Ashida, T. Iida, H. Ishihara, and T. Itoh, Phys. Status Solidi B **243**, 3829 (2006).
[16] T. Kudo and H. Ishihara, Phys. Status Solidi C **8**, 66 (2011).
[17] C. S. Adams and E. Riis, Prog. Quantum Electron. **21**, 1 (1997).
[18] I. Marzoli, J. I. Cirac, R. Blatt, and P. Zoller, Phys. Rev. A **49**, 2771 (1994).
[19] T. Iida and H. Ishihara, Phys. Rev. Lett. **97**, 117402 (2006).
[20] See Supplemental Material at http://link.aps.org/supplemental/10.1103/PhysRevLett.109.087402 for the method and the validity of employed approximation in the calculation, and for further detailed discussions.
[21] R. Bavli, D. F. Heller, and Y. B. Band, J. Chem. Phys. **91**, 6714 (1989).
[22] L. Novotny and B. Hecht, *Principles of Nano-Optics* (Cambridge University Press, 2006), p. 61.
[23] C. Cohen-Tannoudji, J. Dupont-Roc, and G. Grynberg, *Atom-Photon Interactions* (Wiley-VCH, 1992).
[24] S. W. Hell and J. Wichmann, Opt. Lett. **19**, 780 (1994).
[25] D. Braun and A. Libchaber, Phys. Rev. Lett. **89**, 188103 (2002).
[26] S. Albaladejo, M. I. Marques, F. Scheffold, and J. J. Saenz, Nano Lett. **9**, 3527 (2009).
[27] Y. Jiang, T. Narushima, and H. Okamoto, Nature Phys. **6**, 1005 (2010).